lides live on *Hypericum* (Table 1). The absence of cardenolides in these species could be explained if the host plant lacks the necessary precursors or if the beetles do not possess the enzymatic systems needed for such synthesis.

JACQUES M. PASTEELS
DÉSIRÉ DALOZE
Biologie Animale and Chimie Bioorganique, Université Libre de Bruxelles, Brussels 1050, Belgium

References and Notes

1. R. L. Wain, *Annu. Rep. Agric. Hortic. Res. Stn. Univ. Bristol.*, 108 (1943); M. Pavan, *Arch. Zool. Ital.* **38**, 157 (1953); B. P. Moore, *J. Aust. Entomol. Soc.* **6**, 36 (1967); T. H. Hsiao and G. Fraenkel, *Toxicon* **7**, 119 (1969); J. B. Wallace and M. S. Blum, *Ann. Entomol. Soc. Am.* **62**, 503 (1969); M. S. Blum, J. M. Brand, J. B. Wallace, H. M. Fales, *Life Sci.* **11**, 525 (1972).
2. M. Rothschild, *Symp. R. Entomol. Soc. London* **6**, 59 (1972); see table 1.
3. L. Cuénot, *Arch. Zool. Exp. Gen.* **4**, 655 (1896); W. L. Tower, *Carnegie Inst. Washington Publ.* **42**, 320 (1906); A. Ch. Hollande, *Arch. Anat. Microsc. Morphol. Exp.* **13**, 171 (1911); F. M. Jones, *Trans. R. Entomol. Soc. London* **80**, 345 (1932).
4. C. Deroe, unpublished results.
5. Thin-layer chromatography was performed on Macherey-Nagel precoated sil-G plates, using Ch_2Cl_2, methanol, and H_2O (85:14:1) as the eluent.
6. Cardenolides appear as purple spots when sprayed first with 2 percent methanolic *m*-dinitrobenzoic acid and then with 5 percent methanolic KOH [Kedde reagent: D. L. Kedde, *Pharm. Weekbl.* **82**, 741 (1947); I. E. Bush and D. A. H. Taylor, *Biochem. J.* **52**, 643 (1952); M. L. Lewbart, W. Wehrli, T. Reichstein, *Helv. Chim. Acta* **46**, 505 (1963)].
7. For infrared and ultraviolet spectra of cardenolides see K. Yamaguchi, [*Spectral Data of Natural Products* (Elsevier, Amsterdam, 1970)]; for nuclear magnetic resonance spectra of cardenolides see K. Tori and K. Aono [*Shionogi Kenkyusho Nempo* **15**, 130 (1965)].
8. P. Brown, F. Brüschweiler, T. Reichstein, *Helv. Chim. Acta* **55**, 531 (1972); M. B. E. Fayez and S. A. R. Negm, *J. Pharm. Sci.* **61**, 765 (1972).
9. N. K. Kochetkov and O. S. Chizhov, *Adv. Carbohydr. Chem.* **21**, 39 (1966).
10. We thank J. Roba (Continental Pharma) for performing these experiments; the details will be reported elsewhere (J. Roba, in preparation).
11. P. Jolivet and E. Petitpierre, *Ann. Soc. Entomol. Fr.* **12**, 123 (1976).
12. The systematics of the genus *Mentha* is confusing for a nonspecialist because of the existence of numerous hybrids. *Mentha X villosa* Huds is a hybrid of *M. spicata* L. and *M. suaveolens* Ehrh. (= *rotundifolia* auct.). The notomorph used is *alopecuroides* (Hull) [J.-E. De Langhe, L. Delvosalle, J. Duvigneaud, J. Lambinon, C. Vanden Berghen, *Nouvelle Flore de la Belgique, du Grand-Duché de Luxembourg, du Nord de la France et des Régions voisines* (Patrimoine Jardin Botanique National de Belgique, Brussels, 1973)].
13. R. Hegnauer, *Chemotaxonomie der Pflanzen* (Birkhäuser, Basel, 1964–1973).
14. T. V. Zinchenko, *Farm. Zh. Kiev* **14**, 47 (1959). Hegnauer (*13*) reported the occurrence of cardenolides in *Leonurus cardiaca*. In fact, in the original paper the compounds were described as bufadienolides [O. E. Schultz and H. J. Haack, *Arzneim. Forsch.* **11**, 830 (1961)].
15. *Mentha X villosa* (750 g, fresh weight), *R. officinalis* (450 g, dried), and *G. tetrahit* (300 g, dried) were screened for cardenolides by the classical procedure of Reichstein [for example, see M. Rothschild, J. von Euw, and T. Reichstein, *J. Insect Physiol.* **16**, 1141 (1970); *Proc. R. Soc. London Ser. B* **183**, 227 (1973)].
16. J. von Euw, L. Fishelson, J. A. Parsons, T. Reichstein, M. Rothschild, *Nature (London)* **214**, 35 (1967).
17. S. S. Duffey and G. G. E. Scudder, *Can. J. Zool.* **52**, 283 (1974).
18. More details about the qualitative and quantitative variations in the content of cardenolides during the life cycle of these insects will be given elsewhere (J. M. Pasteels and D. Daloze, in preparation).
19. T. Reichstein, *Naturwiss. Rundsch.* **20**, 499 (1967); L. P. Brower and S. C. Glazier, *Science* **188**, 19 (1975).
20. In the animal kingdom, only some toads are known to synthesize true cardenolides, beside the well-known bufadienolides [N. Höriger, H. H. A. Linde, K. Meyer, *Helv. Chim. Acta* **53**, 1503 (1970); N. Höriger, D. Zivanov, H. H. A. Linde, K. Meyer, *ibid.*, p. 2051; Y. Fujii, K. Shimada, T. Nambara, *Chem. Ind. (London)* (1976), p. 614].
21. T. Reichstein and E. Weiss, *Adv. Carbohydr. Chem.* **17**, 65 (1962); I. F. Makarevich, M. Ya Tropp, D. G. Kolesnikov, *Dokl. Akad. Nauk SSSR* **136**, 617 (1961).
22. W. E. Robbins, J. N. Kaplanis, J. A. Svoboda, M. J. Thompson, *Annu. Rev. Entomol.* **16**, 53 (1971).
23. H. Schildknecht, *Angew. Chem. Int. Ed. Engl.* **9**, 1 (1970).
24. We thank T. Reichstein for much helpful advices and for generous gifts of reference compounds. M. Rothschild critically reviewed the manuscript. Thanks are due also to M. Colin and C. Moulard for technical assistance.

20 December 1976; revised 16 February 1977

Freeze-Fractured Purple Membrane Particles: Protein Content

Abstract. *Optical diffraction and image reconstruction can be used to correlate the electron microscope image of the biological membrane with its electron density projection. Such correlation shows that a single purple membrane particle contains 9 to 12 protein molecules—63 to 84 transmembrane alpha helices—a complexity two to ten times greater than that previously suggested for membrane particles.*

Current models of biomembranes show protein intercalated in the lipid bilayer (*1*). The interest in structural details of membrane proteins led to the extensive use of freeze-fracture as a tool to investigate the interior of the membrane bilayer (*2*). This use presupposes that membranes split upon freeze-fracture (*3*) and that the particles seen represent protein (*2*). But the question of what constitutes a "particle" in situ remains unknown, in part because of lack of sufficient structural information about individual membrane-associated proteins.

Recently a membrane protein, bacteriorhodopsin, was described in three dimensions, at 7-Å resolution, by computer analysis of electron diffraction patterns and corresponding micrographs (*4*). Bacteriorhodopsin is a 26,000-dalton polypeptide with covalently bound retinal (*5*) found in *Halobacterium halobium* (*6*). It has an absorption maximum at 570 nm and functions as a light-driven proton pump (*7*). Multiple copies of this protein are associated in vivo in the plasma membrane, in regular arrays that can be visualized by freeze-fracture electron microscopy (*8*).

By combining freeze-fracture with diffraction techniques, we can define the polypeptide content of a particle. We measure particle dimensions and examine packing geometry in freeze-fracture electron micrographs, and obtain the particle lattice by optical filtration. We then verify that the primary structure of the membrane polypeptide after freeze-fracture is the same as in native membrane (that is, no major covalent bonds are broken) and compare the particle image to the filtered lattice. If those lattice points can be superimposed on the previously derived planar electron density projection (*9*), one can relate the particles seen in freeze-fracture to the 7-Å map.

Conventional freeze-fractured preparations (*10*) of light-grown and oxygen-starved cells of *H. halobium* (*11*) reveal quasi-crystalline aggregates of particles in the plane of the membrane half (P face) closest to the cytoplasm (Fig. 1, a and b). Particles can be identified (Fig. 1a) as irregular accumulations of electron-scattering material bordered on one side by a crescent-shaped electron-transparent region (shadow). The complementary half (E face) is devoid of particles but shows a fine lattice at favorable shadow angles.

Particles were selected at random from electron micrographs of fractured *H. halobium* cells at calibrated magnifications of 600,000 ×. Their dimensions were measured with an optical comparator, using lines drawn normal to the shadowing direction. Purple membrane particles were 11.9 ± 2.6 nm wide (mean ± standard deviation, $N = 50$) and adjacent nonaggregated red membrane particles 10.4 ± 1.3 nm wide ($N = 50$; uncorrected for shadowing material). The purple particles were arranged in rows offset from each other by one-half particle width (Fig. 1a). No distinct hexagonal patterns were observed.

Because fractures pass through the cells at many angles, both low-angle and high-angle shadows can be found in a single replica. The low-angle regions, identified by long shadows or minimal Pt-C deposition, are especially useful for detection of particle substructure (Fig. 1b). Scrutiny of such areas reveals subparticle grains of Pt-C occasionally arranged hexagonally (Fig. 1b, circles). Whether this preferential accumulation of Pt-C is primarily due to "decoration" (*12*) or to true shadowing is not known. Our interest, however, was not to exam-

ine the structure of the grain, which is near the limit of Pt-C resolution (*12*), but rather to note its position.

A high-contrast image of the fractured membrane (Fig. 1a) placed in an optical diffractometer produces the type of diffraction pattern shown in Fig. 2a. Measurement of first-order spacings reveals a range of lattice spacings from 4.6 to 4.9 nm. Such spacings are smaller than those derived by diffraction of isolated membrane by about 0.4 to 0.7 nm. Variation is probably due to the uncontrolled tilt of the membrane in bulk-fractured cells because the spacing varies in different directions in the same pattern. When isolated patches of membrane are oriented by attachment to polylysine-treated glass, fractured (*13*), and diffracted, all first-order spots have the same spacing corresponding to 5.3-nm lattice lines and 6.1-nm center-to-center separation (Fig. 2a). Spacings of 6.3 and 6.2 nm have previously been reported from hydrated samples prepared for x-ray diffraction (*8, 13, 14*).

To compare the lattice with the particles, we reconstructed the image from the diffraction pattern and photographed it. A mask punched from the pattern was aligned with the spots in the diffraction plane and used to produce the optically filtered image of the lattice (*15*). The filtered image (Fig. 2b) was transferred to a transparent overlay and directly superimposed on prints of the real image. The comparison revealed that the area within several adjacent unit cells (two to six or more lattice points) could fit within the contours of a single freeze-fracture particle.

Both x-ray diffraction and electron microscopy have shown that a single-unit cell contains three bacteriorhodopsin proteins (*16*) (Fig. 2c). Therefore, a single particle in the freeze-fracture image must be composed of 9 to 12 proteins. The structure of the bacteriorhodopsin protein in three dimensions (*4*) shows that it is composed of seven alpha helices arranged approximately normal to the plane of the membrane (*16*). Thus a single particle can easily accommodate 63 to 84 (7 × 9 to 7 × 12) such helices (Fig. 2d).

Of course, the direct comparison of glucose-embedded, intact, purple membrane sheets to frozen and fractured membranes requires evidence that the particles are proteins whose polypeptides are not significantly altered by freezing and fracturing. We have preliminary evidence that this is the case. Purple membranes adsorbed as monolayers to polylysine-treated glass cover slips (22 by 22 mm) were freeze-fractured (*13*), freeze-dried, and extracted into 0.1 percent sodium dodecyl sulfate for polyacrylamide gel electrophoresis. All bands migrated with the same relative mobility whether they were controls (unbound or bound, unfrozen, unfractured; bound, frozen, unfractured) or experimental bands (bound, frozen, fractured, copper side or glass side). No additional bands were seen following fracturing. That a significant proportion of the membranes had indeed fractured was verified by electron microscopy of shadowed surfaces obtained in parallel experiments.

Freeze-fracture particles are absent from dispersions of amphiphilic lipid bilayers but can be generated by the addition of isolated integral membrane proteins such as bovine rhodopsin (*17*); sarcoplasmic reticulum adenosine triphosphatase (*18*); or erythrocyte gly-

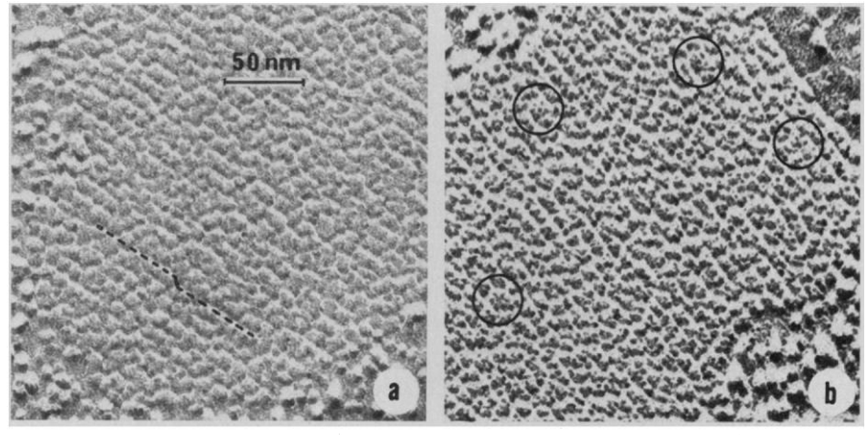

Fig. 1. (a and b) Fracture faces of *Halobacterium halobium* plasma membranes (P faces) showing purple membrane particle aggregates. Cells were scraped from slants, placed on copper supports, and frozen without fixation or cryoprotection in Freon 22. They were fractured at −115°C and 2 × 10^{-6} torr in a Balzers device and shadowed with Pt-C by resistance heating. The shadow direction is from bottom to top (× 220,000). (a) High shadow angle, conventional appearance. Particles are offset by one-half particle width (zigzag line); there is no obvious hexagonal packing of individual particles. (b) Low shadow angle. Subparticle grains show hexagonal arrangements (circles). Four such granules constitute a single particle.

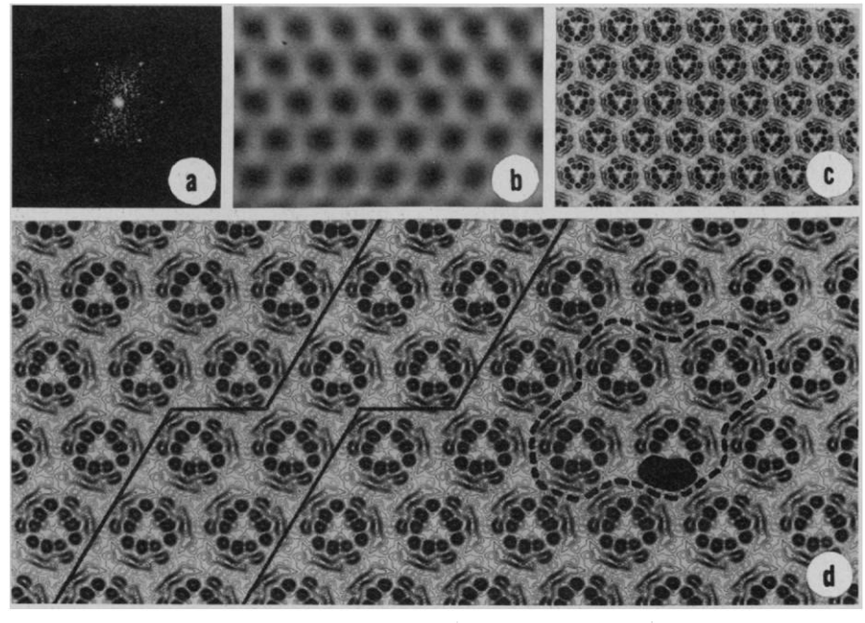

Fig. 2. (a to d) Diffraction-derived images of purple membrane. (a) Diffraction pattern of freeze-fractured purple membrane. Weak second-order spots are visible. (b) Optically filtered image of freeze-fractured membrane. Note the hexagonal arrangement of lattice points. (c) Unwin and Henderson (*9*) electron density projection redrawn and combined to form a collage; printed here at a magnification directly comparable to that in (b). Each lattice point has three molecules and each molecule seven alpha helices (four are shown here as a single smeared band). (d) Collage showing postulated fracture lines (left) and particle structure (right). The blackened area outlines a single bacteriorhodopsin molecule.

cophorin (*19*), glycoprotein fragments (*20*), or band 3 proteins (*21*). From examinations of stoichiometry and correlations of surface reactivity, various authors have suggested that particles may contain dimeric, trimeric, or multimeric associations of polypeptides (*17–22*). In one model system it was calculated that each 8-nm intramembranous particle contained between 10 and 20 tryptic peptide monomers with a combined molecular weight of 45,000 to 85,000 (*20*). Our examinations of "intact" membranes show a degree of association as much as a full order of magnitude greater. However, the presence of 12 protein molecules in a single particle (12 nm in diameter) is not inconsistent with their combined molecular weight ($12 \times 26{,}000 = 312{,}000$) if one recalls that the shadowed ferritin molecule has a diameter of 11 to 12 nm (*23*) and its apoprotein fraction a molecular weight of 480,000 (*24*). For simplicity the purple membrane lipids (25 percent by weight) were not included in the calculation.

Our study provides a clear example of the polypeptide composition of a native membrane particle. The purple membrane helix content is four to five times greater than that calculated in the tryptic peptide reconstitution study (*20*) and a full order of magnitude greater than that of many suggested particle polypeptide contributions. Although we recognize that polypeptide packaging in purple membrane may be unique, such structural complexity may also underlie the other 10-nm particles so commonly found in freeze-fractured biomembranes. If so, simple models of membrane structure, or one-to-one correlations of function and particle occurrence, should be viewed with caution.

KNUTE A. FISHER
WALTHER STOECKENIUS
Cardiovascular Research Institute and *Department of Biochemistry and Biophysics, University of California, San Francisco 94143*

References and Notes

1. S. J. Singer and G. L. Nicolson, *Science* **175**, 720 (1972).
2. D. Branton and D. W. Deamer, *Membrane Structure* (Springer-Verlag, New York, 1972).
3. D. Branton, *Proc. Natl. Acad. Sci. U.S.A.* **55**, 1048 (1966).
4. R. Henderson and P. N. T. Unwin, *Nature (London)* **257**, 28 (1975).
5. D. Oesterhelt and W. Stoeckenius, *Nature (London) New Biol.* **233**, 149 (1971).
6. W. Stoeckenius and R. Rowen, *J. Cell Biol.* **34**, 365 (1967).
7. D. Oesterhelt and W. Stoeckenius, *Proc. Natl. Acad. Sci. U.S.A.* **70**, 2853 (1973).
8. A. E. Blaurock and W. Stoeckenius, *Nature (London) New Biol.* **233**, 152 (1971).
9. P. N. T. Unwin and R. Henderson, *J. Mol. Biol.* **94**, 425 (1975).
10. K. Fisher and D. Branton, *Methods Enzymol.* **32**, 35 (1974).
11. D. Oesterhelt and W. Stoeckenius, *ibid.* **31**, 667 (1974).
12. R. Abermann, M. M. Salpeter, L. Bachmann, in *Principles and Techniques of Electron Microscopy*, M. A. Hayat, Ed. (Van Nostrand Reinhold, New York, 1972), vol. 2, p. 195.
13. K. A. Fisher, *Science* **190**, 983 (1975).
14. R. Henderson, *J. Mol. Biol.* **93**, 123 (1975).
15. A. Klug and D. J. De Rosier, *Nature (London)* **212**, 29 (1966).
16. R. Henderson, *Annu. Rev. Biophys. Bioeng.*, in press.
17. K. Hong and W. L. Hubbell, *Proc. Natl. Acad. Sci. U.S.A.* **69**, 2617 (1972); Y. S. Chen and W. L. Hubbell, *Exp. Eye Res.* **17**, 517 (1973).
18. D. W. Deamer and R. Leonard, in *The Role of Membranes in Metabolic Regulation*, M. A. Mehlman and R. W. Hanson, Eds. (Academic Press, New York, 1972), p. 17; N. T. Malan, R. Sabbadini, D. Scales, G. Inesi, *FEBS Lett.* **60**, 122 (1975); N. Yamanaka and D. W. Deamer, *Biochim. Biophys. Acta* **426**, 132 (1976).
19. C. W. M. Grant and H. M. McConnell, *Proc. Natl. Acad. Sci. U.S.A.* **71**, 4653 (1974).
20. J. P. Segrest, T. Gulik-Krzywicki, C. Sardet, *ibid.*, p. 3294.
21. J. Yu and D. Branton, *ibid.* **73**, 3891 (1976).
22. P. Pinto da Silva and G. L. Nicolson, *Biochim. Biophys. Acta* **363**, 311 (1974).
23. L. W. Labaw and R. W. G. Wyckoff, *ibid.* **25**, 263 (1957).
24. P. M. Harrison and T. Hofmann, *J. Mol. Biol.* **4**, 239 (1962).
25. We thank K. Yanagimoto for technical help. A portion of this work was presented at the Eighth Western Regional Meeting of Electron Microscopists in San Francisco, California, on 11 February 1977. Supported by NIH training grant HL 05251 (K.A.F.) and PHS grant HL 06285.

27 December 1976; revised 28 February 1977

Intravenous Naloxone Administration in Schizophrenia and Affective Illness

Abstract. *Fourteen schizophrenic patients and five patients with affective disorders were given naloxone (0.4 to 10 milligrams) or placebo intravenously in a double-blind fashion. Physicians' ratings of hallucinations, mannerisms and posturing, conceptual disorganization, psychosis, and mood did not change significantly. A single item, unusual thought content, improved significantly on the naloxone day compared to the placebo day. There was no improvement in mood in affectively ill patients rated either by themselves or by physicians. Naloxone did not markedly improve any patient studied, which suggests that the acute blockade of opiate receptors is not associated with global improvement in psychotic symptomatology.*

The recent discoveries of the opiate receptor and endogenous polypeptides that bind to that receptor (*1*) have initiated a search for a peptidergic neuronal system that may influence a variety of behaviors. In humans, endogenous substances that bind to opiate receptors (endorphins) have been demonstrated in cerebrospinal fluid (CSF), brain, and peripheral blood (*2, 3*). Reports of psychotomimetic actions of narcotics and certain narcotic antagonists have led to the suggestion that some behavioral disorders may be associated with an excess of natural opiatelike compounds at specific sites in the central nervous system.

The link between psychotic behavior and endorphins has been suggested by the resemblance of behavioral states induced by endorphins in rats to human catatonia and to neuroleptic-induced catalepsy (*4, 5*). In one study, the investigators reported that reduced symptoms of schizophrenia were associated with a decreased level of endorphin in CSF (*6*). They also found elevated endorphin levels in the CSF of manic patients. In further study linking opiates to mood disorders, cyclazocine, a mixed narcotic agonist-antagonist, had a clinical antidepressant action (*7*). Perhaps the most provocative suggestion is the recent report that naloxone reduces or even eliminates temporarily the auditory hallucinations of chronic schizophrenics (*8*). Naloxone is a pure narcotic antagonist that has been shown to reverse and block opiate effects including analgesia, respiratory suppression, and psychotomimetic and other side effects (*9*). Naloxone has been shown to be effective in reversing the effects induced by endorphins as well (*3, 4*). If excessive endorphin is associated with human behavioral disorders, naloxone would be expected to promptly reverse relevant symptomatology. In this report, the possible antipsychotic and mood-altering effects of naloxone are tested in patients with schizophrenia and affective illness.

Patients participating in this study were all seriously ill inpatients at the National Institute of Mental Health. All were voluntary patients and had signed informed consent. The clinical characteristics of this population are described in Table 1. Naloxone or a matched volume of physiological saline was administered intravenously in a randomized double-blind fashion. The following items were rated on a severity scale of 1 to 7 (not present to severe): hallucinations, mannerisms and posturing, conceptual disorganization, unusual thought content, psychosis, and the mood variables of depression, elation, and dysphoria (*10*). These variables were chosen in order to evaluate the possible antipsychotic and antidepressant effects cited earlier. Blind ratings were performed before and 1 hour after each injection. In addition, each patient was interviewed for 15 min-